molecular pharmaceutics

Article

WELL-DEFINED STAR-SHAPED POLYGLUTAMATES WITH IMPROVED PHARMACOKINETIC PROFILES AS EXCELLENT CANDIDATES FOR BIOMEDICAL APPLICATIONS

Aroa Duro-Castano, Richard M. England, David Razola, Eduardo Romero, Marta Oteo-Vives, Miguel Angel Morcillo, and Maria J. Vicent

Mol. Pharmaceutics, **Just Accepted Manuscript** • DOI: 10.1021/acs.molpharmaceut.5b00358 • Publication Date (Web): 10 Sep 2015

ACS Publications

Molecular Pharmaceutics is published by the American Chemical Society. 1155 Sixteenth Street N.W., Washington, DC 20036

WELL-DEFINED STAR-SHAPED POLYGLUTAMATES WITH IMPROVED PHARMACOKINETIC PROFILES AS EXCELLENT CANDIDATES FOR BIOMEDICAL APPLICATIONS

*Aroa Duro-Castano,[1] Richard M. England,[1] David Razola,[2] Eduardo Romero,[2] Marta Oteo-Vives,[2] Miguel Angel Morcillo,[2] María J. Vicent[1]**

1. Polymer Therapeutics Lab., Centro de Investigación Príncipe Felipe (CIPF), Av. Eduardo Primo Yúfera 3, Valencia 46012, Spain.

2. Biomedical Applications of Radioisotopes and Pharmacokinetics Unit, CIEMAT, Av. Complutense 40, Madrid 28040, Spain

KEYWORDS ((Ring-opening polymerization, polypeptides, star-shaped polymers, polyglutamates, NCA polymerization, polymer therapeutics, drug delivery))

ABSTRACT

There is a need to develop new and innovative polymer carriers to be used as drug delivery systems and/or imaging agents owing to the fact that there is no universal polymeric system that can be used in the treatment of all diseases. Additionally, limitations with existing systems such as lack of biodegradability and biocompatibility inevitably lead to side effects and poor patient compliance. New polymer therapeutics based on amino acids are excellent candidates for drug delivery, as they do not suffer from these limitations. This article reports on a simple yet powerful methodology for the synthesis of 3-arm star-shaped polyglutamic acid with well-defined structures, precise molecular weights (MW) and low polydispersity (Đ = <1.3). These were synthesized by ring opening polymerization (ROP) of N-carboxyanhydrides (NCA) in a divergent method from novel multifunctional initiators. Herein, their exhaustive physicochemical characterization is presented. Furthermore, preliminary *in vitro* evaluation in selected cell models, and exhaustive *in vivo* biodistribution and pharmacokinetics highlighted the advantages of these branched systems when compared with their linear counterparts in terms of cell uptake enhancement and prolonged plasma half-life.

1. Introduction

There has been a considerable effort devoted to the development of new and more versatile polymeric architectures with specific and predictable properties to be used as targeted drug delivery systems.[1] Such desirables features in these materials include; adjustable molecular weights (higher MW to enhance passive targeting by the Enhanced Permeability and Retention (EPR) effect),[2-4] predictable structure and conformation in solution, lower heterogeneity, and greater possibility for multivalency. Nevertheless, the design and synthesis of new polymeric constructs of relevant MW, together with their physicochemical characterization, conformational

studies, and especially their potential for biological applications still remain to be fully exploited in this area. To this aim, polypeptide-based architectures can be considered suitable aspirants.

The ring opening polymerization (ROP) of α-amino-*N*-carboxyanhydrides (NCAs)[5-7] can be considered an excellent method to produce a wide variety of polypeptide architectures including homopolymers, copolymers, block copolymers, and branched systems that do not exist naturally, on multigram scale with relative ease. Since the first NCA synthesis by Leuch and coworkers[8-10] many methodologies have been described with the aim of improving and overcoming the inherent limitations of this polymerization technique, as reviewed in the following excellent literature.[5-7] Among them, the use of high vacuum techniques (HVT),[11] amine hydrochloride salts,[12] heavy metal catalysts,[13] hexamethyldisilazanes (HMDS)[14] as well as by means of optimization of reaction conditions (pressure, temperature etc.)[15] can be considered. Nevertheless, all methods have their own limitations. Previously in our group we have reported the use of primary amine tetrafluoroborate (BF_4) salts as an improvement over the use of hydrochloride salts. This potent alternative is based on the non-nucleophilicity of the BF_4 salts allowing the synthesis of well-defined polyglutamates (amongst other polypeptides), on multigram scale and with low polydispersity (Đ<1.3), adjustable MW, controlled chain end functionality and adequate stereoselectivity, ideal features for biomedical applications.[16,17]

Star polypeptides are branched polymers, which consist of various linear chains linked to a central core. There are two main synthetic strategies described: the core-first approach (or multifunctional initiators or divergent approach) and the arm-first approach (or the use of multifunctional linking agents, or convergent approach). The core-first approach is based on the use of a multifunctional initiator that simultaneously initiates the polymerization of several arms while in the arm first approach the living arms are linked to a multifunctional agent. Besides

those technologies, there is a recent classification including another strategy based on the reaction of living macroinitiators (MI) (or macromonomers) with a multifunctional cross-linker to provide the so-called core cross-linked star (CCS) polymers.

Various polypeptide-based star polymers have been synthesized over the years. For example, Klok *et al*.[18] used perylene derivatives with four primary amine groups as initiators to lead 4-arm PBLG and PZLL and Inoue *et al*.[19-20] used hexafunctional initiators for the synthesis of 6-arm PBLG star polymers both taking profit of the NCA polymerization techniques. Other examples are provided from the work of Aliferis *et al*.[21] who used 2-(aminomethyl)-2-methyl-1,3-propanediamine as a trifunctional initiator for the synthesis of P(BLL-*b*-BLG)$_3$ 3-arm star-block co-polypeptides; or the studies of Karatzas *et al*.[22] in the synthesis of 4-arm (PEO-*b*-PBLG) hybrid star block co-polymers using 4-arm PEO stars end-functionalized with primary amines as initiators for the polymerization of BLG-NCA among others. More recent examples include the use of dendritic cores based on poly(ethylene imine) (PEI),[23] poly(propylene imine) (PPI)[24-26] or poly(amidoamine) (PAMAM)[27] as initiators. All these examples are based on the use of the amine initiated NCA approach with its inherent limitations that could lead to star polymers with either low molecular weight or with very broad molecular weight distributions. The use of HVT from Hadjichristidis group can be seen as a suitable solution,[21-22] however, the requirement of complex equipment is always a disadvantage in order to develop a versatile synthetic procedure.

Despite the growing interest in the development of hybrid and peptide-based star polymers as prospective advanced materials for biological applications, only recently, they have been explored as drug delivery systems. For instance, Sulistio *et al*.[28-30] synthesized peptide-based CCS polymers composed of PLL arms emerging from a poly(L-cysteine) (PLC) able to

entrap hydrophobic drugs, such as the anti-cancer drug pirarubicin. Xing *et al.*[31] prepared CCS polymers using $MeOPEG_{1900}$-NH_2 as a macroinitiator for ROP cysteine and benzyl glutamate NCA derivatives which resulted in the formation of nanogels able to entrap the hydrophobic drug indomethacin. Also, the PPI initiated multi-arm stars from Byrne *et al.* were efficiently loaded with rhodamine B.[25]

Taken into account all the stated above, herein, we pursued the development of novel star-shaped architectures for their use as polymeric carriers by means of a simple NCA polymerization methodology. Our approach does not require of neither complex and expensive equipment nor low temperatures, but is capable to yield star-shaped polypeptides with low polydispersities in a relatively short time and in a variety of MW including high molecular mass. As the applicability of these novel constructs will be first demonstrated as nanocarriers, their *in vitro* validation in selected cell models was also performed, in terms of biodegradability, cell viability and cellular uptake. Furthermore, their *in vivo* biodistribution profile and pharmacokinetics in comparison with their linear polymeric counterpart is also presented.

2. Experimental Section

Materials

All chemicals were reagent grade, obtained from Aldrich and used without further purification, unless indicated otherwise. H-L-Glu(OBzl)-OH, was obtained from Iris Biotech. Phenazinemethosulfate (PMS) were supplied by Sigma (Sp). Dulbecco's Modified Eagle's Medium (DMEM), Leibovitz, Phosphate buffer saline (PBS), Foetal bovine serum (FBS) and Trypsin, were provided from Gibco. (3-(4,5-dimethylthiazol-2-yl)-5- (3-carboxymethoxyphenyl)-2-(4-sulfophenyl)-2H-tetrazolium) (MTS) was supplied by Promega (Sp). DO_3AtBu was purchased from Chematec. ^{111}In was obtained from Covidien Spain, S.L. All

solvents were of analytical grade and were dried and freshly distilled. Deuterated chloroform-*d1*, DMSO-*d6*, DMF-*d7* and D_2O were purchased from Deutero GmbH. Preparative SEC was performed using Sephadex G-25 superfine from GE as well as PD MiniTrap G-10 ™ columns containing 2.1 mL of Sephadex™ G-10. Ultrafiltration was performed in a Millipore ultrafiltration device fitted with a 1, 3, or 10 kDa molecular weight cut off (MWCO) regenerated cellulose membrane (Vivaspin ®)

Characterization techniques

NMR spectroscopy. ^{1}H and ^{13}C-NMR spectra were recorded on a Bruker AC 300 at room temperature and at a frequency of 300 and 75 MHz respectively and analyzed using the MestreNova 6.2 software.

Dimethylformamide (DMF) gel permeation chromatography (GPC). For SEC measurements in DMF containing 1g/L of lithium bromide as an additive, an Agilent 1100 series system was used with a flow rate of 1 mL/min at 70 °C as an integrated instrument, including three HEMA-based columns ($10^5/10^3/10^2$ Å porosity) from MZ-Analysentechnik GmbH, Viscoteck TDA^{TM} 302 triple detector 87 with UV detection coupled, and Calibration was achieved with well-defined poly(methyl methacrylate) (PMMA)/DMF standards, provided by Polymer Standards Service (PSS)/Mainz Germany.

Circular Dichroism (CD). CD Spectroscopy was performed with a J-815 CD Spectrometer (JASCO Corporation) using a Peltierthermostated cell holder (PTC-423, JASCO Corporation) with a recirculating cooler (JULABO F250, JASCO Corporation). A nitrogen flow (~2.7 L/min) was lead through the spectrometer and controlled with a nitrogen flow monitor (Afriso Euro-Index).The samples were dissolved in HFIP for protected and PBS pH=7.4 for deprotected samples and diluted to a concentration of 0.1 mg/mL. Samples were measured repeatedly (n=3)

in a quartz cuvette with d= 0.1 cm at 20 °C for HFIP samples and 37 ºC for PBS dissolved samples. Obtained molar ellipticities were plotted as mean residue ellipticity.

Dynamic Light Scattering (DLS). DLS measurements were performed at 25 °C using a Malvern ZetasizerNanoZS instrument, equipped with a 532 nm laser at a fixed scattering angle of 173°. Polymer conjugate solutions (0.2 mg/mL) were prepared in PBS pH= 7.4. The solutions were sonicated for 10 min and filtered through a 0.45 μm cellulose membrane filter. Size distribution by volume was measured (diameter, nm) for each conjugate per triplicate with n>3 measurements.

Protocols

Monomer Synthesis: Synthesis protocol followed as that reported in Conejos-Sanchez *et al.*[16-17] Detailed protocol can be found in Supporting Information (SI).

Initiator Synthesis: For clarity reasons, only the ethyl-based initiator will be included in the manuscript. The others are included in the Supporting Information.

a) Synthesis of 1,3,5-Tri-tert-butyl ((benzenetricarbonyltris(azanediyl)) tris(ethane-2,1-diyl))tricarbamate. In a two-neck round bottom flask fitted with a stirrer bar, and a N_2 inlet and outlet, 500 mg of 1,3,5-benzenetricarbonyl trichloride (1.88 mmol, 1 equivalent (eq.)) was dissolved in 12 mL of anhydrous THF. N,N',N''-diisopropylethylendiamine (DIEA) (803.31 mg, 6.22 mmol, 3.3 eq.) was added to the reaction mixture followed by drop-wise addition of N-Boc-ethylendiamine (1.34 g, 6.22 mmol, 3.3 eq.) over a period of 10 min. The reaction was then left to proceed for 2 hours. After that time, the solvent was completely removed under vacuum. The product was re-dissolved in chloroform and washed 3 times with deionized water (ddH_2O), and 3 times with acidic water (pH~3). Finally, the organic phase was isolated under vacuum and the

product was recrystallized 3 times from THF/Methanol/Hexane yielding a white crystalline solid. The product was then dried under high vacuum and stored at -20 °C.

Yield: 82 %. ^{1}H NMR (300 MHz, DMSO) δ 8.68-8.65 (m, 3H), 8.41 (s, 3H), 6.92-6.88(m, 3H), 3.34-3.31 (m, 6H), 3.16-3.13 (m, 6H), 1.37 (s, 27H).^{13}C NMR (75 MHz, $CDCl_3$) δ 166.80 (C=O), 156.84 (C=O), 134.58 (C_{Ar} quaternary), 128.47 (CH_{Ar}), 79.57 (C quaternary), 40.93 (CH_2), 40.43 (CH_2), 28.45 (CH_3).

b) Synthesis of 1,3,5-(benzenetricarbonyltris(azanediyl))triethanamonium BF_4 salt. In a round bottom flask fitted with a stirrer bar and a stopper, 200 mg of 1,3,5-Tri-tert-butyl ((benzenetricarbonyltris(azanediyl)) tris(ethane-2,1-diyl))tricarbamate (0.33 mmol, 1 eq.) was dissolved in dichloromethane. Afterwards, 3.3 eq. of tetrafluoroboric acid diethyl ether complex, $HBF_4.Et_2O$, (179 mg, 150 µL), was added to the solution leading to the instantaneous formation of a white solid. The precipitate was filtered off and recrystallized three times from THF/methanol/hexane. The product was then dried under high vacuum and stored at -20 °C.

Yield: 98 %. ^{1}H NMR (300 MHz, D_2O) δ 8.32 (s, 3H), 3.72-3.68 (m, 6H) 3.25-3.21 (m, 6H).^{13}C NMR (75 MHz, D_2O) δ 169.45 (C=O), 134.38 (C_{Ar} quaternary), 129.36 (C_{Ar}), 39.23 (CH_2), 37.52 (CH_2).^{19}F-NMR: -150.48 (BF_4). MALDI-TOF: 337.1709 [M^{+1}]

St-PBLG Polymer Synthesis: As for Conejos-Sanchez et al. [16-17] with slight variations, briefly, γ-Benzyl L-glutamate N-carboxyanhydrides (0.5 g, 1.9 mmol) was added to a Schlenk tube fitted with a stirrer bar, a stopper and purged with 3 cycles of vacuum/Ar, and dissolved in 5 mL of the freshly purified solvent. The 3-arm initiator was added and the mixture was left stirring at 4 °C for 3 days under inert atmosphere. Finally, the reaction mixture was poured into a large excess of cold diethyl ether leading to a white polymer after isolation. Yield: 70-90 %. ^{1}H-NMR (300

MHz, DMF, δ) 8.58 (s, xH), 7.42 (s, 5H), 5.19 (s, 2H), 4.21 (s, 1H), 2.81 (s, 2H), 2.45 (s, 2H).^{13}C-NMR (300 MHz, DMF, δ) 175.94 (s), 172.26 (s), 162.77-162.18 (m), 161.98 (s), 136.76 (s), 128.87-127.75 (m), 66.05 (s), 57.13 (s), 35.41-34.17 (m), 32.48 (s), 30.84, 30.30 -29.04 (m), 27.28 (s), 25.99 (s). x: DP obtained/3 arms

Deprotection: different methods were followed depending on the initiator used: acid conditions were applied when ethyl and hexyl based initiators were used. On the other hand, basic conditions were applied for DOOA (3,6-dioxa-8-octaneamine), and cystamine based initiators synthesis. Briefly:

Deprotection of St-PBLG with HBr in trifluoroacetic acid (TFA): in a round bottom flask fitted with a glass stopper and a stirrer bar, 50 mg of St-PBLG (0.23 mmol, 1 eq. glutamic acid unit, GAU) were dissolved in TFA. Once dissolved, 2 eq. of HBr (48 % v/v) per carboxyl group were added drop wise, and the mixture was stirred for five hours. *Note: For big scale deprotection of St-PBLG, 16 hours were applied for full deprotection. Then, the solution was poured into a large excess of cold diethyl ether leading to a white solid after isolation.

Deprotection of St-PBLG in basic conditions: in a round bottom flask, 40 mg of benzyl protected St-PBLG (0.183 mmol, 1 eq. GAU) was dissolved in 16 mL of THF. The solution was cooled down to 4 °C and 2 eq. of NaOH per carboxylic group of the polypeptide block (14.7 mg, 0.369 mmol) were added in 2 mL of ddH_2O. The mixture was stirred for 16 hours. Finally, THF was removed and the residue was diluted with ddH_2O, concentrated and purified by ultrafiltration (Vivaspin®, MWCO= 3000 Da) or by size exclusion columns (G25).

Yields: 75-86 %. ^{1}H-NMR (300 MHz, D_2O, δ) 8.2 (s, xH), 4.31-4.26 (m, 1H), 2.38-2.14 (m, 2H) 2.10-1.80 (m, 2H) 2.10-1.80 (m, 2H). x: DP obtained/3 arms

Note: depending on the initiator used, the corresponding signals of the Ethyl, Hexyl, or DOOA were also present.

Conjugation of Oregon Green Cadaverine to linear and star PGA: In a round two necked bottom flask fitted with a stirrer bar and two septums, 29 mg of PGA (linear or star) (0.225 mmol GAU, 1 eq.) was weighed and dissolved in 1.5 mL of dry DMF under N_2 flow. Of N,N'Diisopropylcarbodiimide (1.12 µL) and DIC (0.85 mg, 0.00674 mmol, d= 0.806 g/mL, 0.03 eq.) were added and the reaction was left to proceed for 5 min at room temperature. Afterwards, Hydroxybenzotriazole, HOBt (1 mg, 0.00674 mmol, 0.03 eq.) was added directly. The reaction was then left to proceed for 10 min before Oregon Green Cadaverine (1 mg, $2.25 \cdot 10^{-3}$ mmol, 0.01 eq.) was added. The pH was adjusted to 8 by adding ~100 µL of DIEA. The mixture was left stirring overnight protected from light. Finally, the solvent was removed under vacuo at room temperature and the product was dissolved in 300 µL of water and then adding ~50 µL of $NaHCO_3$ 1M. The solution was purified by Sephadex PD10 column eluting with distilled water. The Oregon Green loading was calculated by fluorescence using a Victor^{2}Wallace^{TM} plate reader with excitation filter of 490 and emission filter of 535. A calibration curve with Oregon green was first performed. Yield: 95 %. OG loading: 0.8 mol glutamic acid unit.

Conjugation of $DO_3AtBu\text{-}NH_2$ to St-PGA: In a two-neck round bottom flask fitted with a stir bar and two septums, 300 mg (of St-PGA (SE2), 110 GAU, 2.32 mmol GAU, 1 eq.) was dissolved in 20 mL of anhydrous DMF under nitrogen flow. Then, 53 µL of DIC (88 mg, 0.70 mmol, 0.3 eq.) were added and the reaction was left to proceed for 5 min at room temperature. Afterwards, HOBt (94 mg, 0.70 mmol, 0.3 eq.) was added directly. The reaction was then left to proceed for 10 min before $DO_3AtBu\text{-}NH_2$ (282 mg, 0.46 mmol, 0.2 eq.) was added for 20 % modification. The pH was adjusted to 8 by adding ~100 µL of DIEA. The mixture was left stirring for 48 hours

at room temperature and protected from light. Finally, the solvent was partially removed under vacuo, precipitated into a large excess of cold acetone, filtered off and washed three times with cold acetone. A pale yellow solid was obtained after drying. The percentage of modified GAU was calculated as 20 % mol GAU, according to the tBu groups signal at 1.4 ppm in comparison with the alpha proton of PGA backbones in ^{1}H-NMR spectra. Conjugation efficiency: 100 %. Yield: 75 %.

Deprotection of DO_3A tBu-NH_2: The construct was dissolved in CH_2Cl_2/TFA (3/2, v/v) mixture and left under vigorous stirring for 16 hours at room temperature. After that time, the solution was precipitated by pouring into a large excess of cold diethyl ether. Pale yellow solid was obtained after filtering, washing with diethyl ether and drying under vacuum. Complete deprotection was achieved as confirmed by ^{1}H-NMR. Yields: 90 %.

Labelling with ^{111}In: St-PGA-DO_3A-^{111}In was prepared by dissolving 51.3 mg of St-PGA-DO_3A in deionized water to a final concentration of 10 mg/mL. Then, 0.25- 0.5 mL of this dissolution was transferred into a microwave tube and the pH was adjusted to 3.5-4 by adding HEPES buffer and HCl 2 M. Next 7-27 MBq of $^{111}InCl_3$ in HCl 0.05 M was added and the reaction mixture heated at 90 ºC for 5 min by using a laboratory microwave with monomodal radiation (Discover Benchmate, CEM). After that, the reaction mixture was cooled down with nitrogen gas. The reaction was stopped after 5 min at room temperature by the addition of 50 µL of 50 mM ethylenediaminetetraacetate acid (EDTA). St-PGA-DO3A-^{111}In was purified from unreacted ^{111}In-EDTA by exclusion molecular chromatography cartridge (Bio Gel P-6, BioRad) using phosphate buffered saline (pH=7) as eluent, at flow rate 0.5 mL/min. The elution profile was determined by fractionating, 0.77 mL per fraction, and measuring each with a dose calibrator (VDC 405, Veenstra). Radiochemical yield (RY) was calculated as percentage of the activity in

each fraction eluted from the molecular exclusion cartridge of the total activity purified and corrected for the decay.

Degradations with Cathepsin B: St-PGA was degraded in presence of the lysosomal enzyme cathepsin B as its linear counterpart. To test the profile and ratio of the degradation of the polymers by cathepsin B, solutions of the polymers (3 mg/mL) were prepared. 3 mg exactly were weighed and 700 µL of acetate buffer 20 mM, pH 6, 100 µL of EDTA 2mM, 100 µL of DTT 5mM were added. Finally, 6.25 units of Cathepsin B (100 µL of a solution of 25 units of cathepsin B in 400 µL of acetate buffer pH 6 20 mM were added. Cathepsin B needs pH 6 to be active, the DTT solution is added to activate Cathepsin B and the solution of EDTA was added to complex the free cations (mainly Ca^{2+} that inactivates cathepsins). Once the solutions were prepared, aliquots of 100 µL were picked at different time points (t= 0, 0.5, 1, 2, 4, 8, 24, 48 and 72 hours) after homogenization of the solutions. Meanwhile, the samples were kept at 37 ºC under stirring. The aliquots taken were frozen and later analyzed by GPC. To evaluate the mass of the conjugates, 100 µL of 3 mg/mL conjugate solution in PBS was injected in the GPC using two TSK Gel columns in series G2500 PWXL and G3000 PWXL with a Viscoteck TDA^{TM} 302 triple detector 87 with UV detection coupled. The mobile phase used was PBS 0.1 M, flow 1 mL/min

Cell culture protocols: Human umbilical vein endothelial (HUVEC) cells were cultured in Medium 200 supplemented with Low Serum Growth Supplement (LSGS). Human derived neuroblastoma (SHSY5Y) cells were cultured in Dubelcco's Modified Eagle Medium (DMEM) supplemented with L-glutamine and Foetal Bovine Serum (FBS). Cells were maintained at 37 °C in an atmosphere of 5 % carbon dioxide and 95 % air. Medium was replaced every 2-3 days and underwent passage once weekly when 80 % of cell confluence was reached.

MTS assay for cell viability determination: Cells were seeded in sterile 96-well microtitre plates at a cell density of 35000 cell/cm^2 for SHSY5Y and 1260 cell/cm^2 for HUVEC. Plates were incubated for 24 hours and compounds (0.2 μm filter sterilized) were then added to give a final concentration of 0-3 mg/mL. After 72 hours of incubation, [3 - (4,5-dimethylthiazol-2-yl) - 5 - (3-carboxymethoxyphenyl) - 2 - (4-sulfophenyl)2H - tetrazolium] (MTS) (10 μL of manufacturer solution) was added to each well, and the cells were incubated for a further 2 hours. Mitochondrial dehydrogenase enzymes of viable cells converted MTS tetrazolium into a colored formazan product. The optical density of each well was measured at 490 nm. The plates were read spectrophotometrically using a Victor^2 Wallace^{TM} plate reader. The absorbance values were represented as the percentage of cell viability taken as 100 % cell viability of untreated control cells.

Cellular uptake by flow cytometry of OG-labeled polymers in SHSY5Y cells: SHSY5Y cells were seeded in 6-well plates at a density of 35000 cell/cm^2 (1 mL cell suspension per well) and allowed to adhere for 24 hours. In the binding experiments conducted at 4 °C, the cells were pre-incubated at this temperature for 30 min prior to start the experiment. For both experiments, 4 ºC, and 37 ºC, the cathepsin B inhibitor CA-074 (0.4 μL from a solution of 5μM to reach a final concentration of 2 μM) was added 30 min before the addition of the conjugate. Then, 10 μL of OG-labeled polymer (0.01 mg OG/mL) were added at different time points from 0 to 300 min meanwhile the cells were incubated either at 37°C or 4°C for each experiment. Finally, the cells were placed on iced in order to stop the energy dependent mechanisms and washed twice with cold PBS-BSA 0.1 %. (PBS supplemented with Bovine Serum Albumin (BSA)). Then the cells were suspended in 0.5 mL of cold PBS by the use of a scraper. Finally, the cell pellet was placed in flow cytometer tubes. Cell-associated fluorescence was then analyzed using a Becton

Dickinson FACS Calibur cytometer (California, USA) equipped with an argon laser (488 nm) and emission filter for 550 nm. Data collection involved 10,000 counts per sample, and the data were analyzed using CELLQuest^{TM} version 3.3 software. Data are expressed by plotting the cell-associated fluorescence, which is the result of the % of positive cells by multiplied by the mean fluorescence. CAF= % positive cells*mean fluorescence/100. Also, the % positive cells is shown. Cells incubated without polymer were used as control in order to account for the background fluorescence (cell autofluorescence).

Confocal fluorescence microscopy: Live-cell imaging. For live-cell imaging, SHSY5Y cells were seeded at a density of 35000 cell/cm^2, on glass bottom culture dishes (1 cm^2 Petri plate) and allowed to seed for 24 hours at 37 ºC. The experiment was performed following a pulse-chase mode at 37 ºC. First, the cathepsin B inhibitor CA-074 (0.4 μL from a solution of 5 μM to reach a final concentration of 2 μM) was added 30 min prior the addition of the St-PGA-OG. Then, 10 μL of OG-labeled polymer (0.01 mg OG/mL) were added and the cells were incubated for 2 hours at 37 °C (pulse). The medium was removed and the cells were washed twice with PBS. 1 mL of medium containing 2 μM of the CA-074 inhibitor was then added, and the cells were incubated for 4 hours at 37 ºC (chase). 30 min before washing the cells with PBS-BSA 0.1 %, the nuclear marker Hoetch (1 μL from a solution 5 mM), and the lysosomal marker Lysotracker Red (0.75 μL from a solution of 100 μM) were added in order to identify possible co-localizations and therefore establish an endocytic pathway. Finally, the cells were washed with PBS-BSA 0.1 %. Then, the glass removed and placed on the microscope chamber with fresh media containing 2 μM of CA-074 inhibitor. Samples were analyzed under the microscope and images were captured after excitation of the fluorophore. Images were captured with an inverted DM IRE2 microscope equipped with a λ-blue 60X oil immersion objective and handled with a TCS SP2

system, equipped with an Acoustic Optical Beam Splitter (AOBS). Excitation was performed with an argon laser ((OG 496 nm) and HeNe laser (Lysotracker Red 594 nm), and blue diode (Hoetch 405 nm). Images were captured at an 8-bit grey scale and processed with LCS software (version 2.5.1347a, Leica Germany) containing multicolor, macro and 3D components. Control cells that followed the same incubation time were also analyzed to establish the autofluorescence, as well as cells treated only with Hoetch or Lysotracker Red.

Statistical Analysis. Values obtained from the experiments were analyzed using one-way ANOVA. In all cases, we considered differences to be significant when $p^{***} < 0.001$; $p^{**} < 0.01$; $p^{*} < 0.05$; ns: non-significant.

Biodistribution and pharmacokinetics (PK): Biodistribution and pharmacokinetics of [^{111}In]-St -PGA-DO_3A was evaluated by analysis of radioactivity. FVB/NJ adult mice (CIEMAT Laboratory Animals Facility, Madrid, Spain) were housed on a 12-hour light and 12-hour dark cycle. Free access to food and water was allowed at all times. All animal protocols were approved by the Institutional Animal Care and Use Committee at CIEMAT (Madrid, Spain). For the pharmacokinetics and biodistribution study, 30 mice (5 mice at each time point for each compound, 23±1g of body weight) were anesthetized with 1.5 % isofluorane, and between 0.05-2 MBq of [^{111}In]-St -PGA-DO_3A (0.5-20 µg compound/g body weight) per mouse was injected intravenously through the tail vein. At 0.5, 1, 2, 4, 8 and 24 hours following injection, blood samples were obtained from mice by terminal bleeding via cardiac puncture following isofluorane anaesthesia; organs (lungs, heart, spleen, kidneys, liver and brain) and tissues (muscle, fat) were isolated, rinsed with normal saline, weighted, and radioactivity was measured using the Cobra II auto-gamma counter. The blood samples were centrifuged (10 min, 3000 rpm) and the supernatant of plasma was transferred to a new eppendorf tube for later analysis. The

percentage injected dose per gram tissue (% ID/g) was calculated by comparison with standards taken from the injected solution for each animal. The data were expressed as the mean ± standard deviation.

3. Results and Discussion

3-arm star shaped polyglutamates have been synthesized throughout a facile and versatile methodology based on the use of ammonium tetrafluoroborate (BF_4) salts as initiators for NCA polymerization[16-17] to yield well-defined carriers with potential biological applications showing tunable MW and low polydispersities (Scheme 1). Remarkably, this methodology allow us to reach such described constructs in a high batch to batch reproducibility, within reasonable reaction times and without the need of using complex or expensive equipment as for HVT, or the incorporation of metal catalysts that, if not carefully removed, could compromise the desired bio-applications.

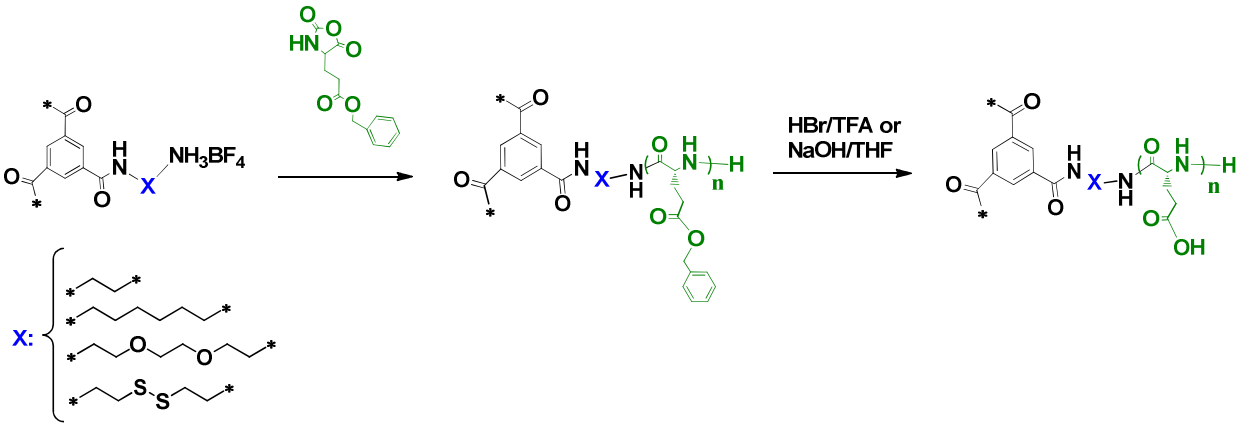

Scheme 1. a) Schematic representation of the NCA polymerization using star-shaped initiators.

The control in the initiation step that this newly described methodology offers is key to the synthesis of branched polymers with predictable molecular weights and low polydispersities. By using a variety of multifunctional amine initiators in their BF_4 salt form to ring-open polymerize the benzyl-L-glutamate NCA results in a fast and homogeneous initiation and efficient propagation to achieve well-defined architectures. To this aim we synthesized four different multifunctional 3-arm initiators, including one that contained disulfide bonds within the arms. In the presence of a reducing agent (GSH or DTT) the star could then be disassembled into the individual arms. This novel initiator for polypeptide synthesis enables the characterization of the individual arms to ensure similar chain length resulting from a living polymerization and efficient initiation. In all the cases, the synthesis of the initiator was carried out starting from the multifunctional core 1,3,5-benzenetricarbonyl trichloride, to which, the mono-Boc protected diamines, N-Boc-ethylendiamine N-Boc-1,6-hexanediamine, 1-(t-Butyloxycarbonyl-amino)-3,6-dioxa-8-octaneamine (N-Boc-DOOA), and N-Boc-cystamine were efficiently coupled in a simple and clean reaction. The mono-Boc protected 3-arm initiator precursors were carefully purified to avoid di- or mono-functional cores that would lead to unwanted mixtures of 1- and 2-arm star polymers. Once purified, the BF_4 ammonium salt initiators were obtained simply by the removal of the Boc groups using tetrafluoroboric acid.

We have explored the versatility of the BF_4 salts based methodology by polymerization of OBzl-L-Glu NCA to yield 3-arm star shaped polyglutamates with different molecular weights ranging from 15000-50000 Da (Table 1, Figure 1) and polydispersities in the range of 1-1.3 independently of the initiator used. This appears to suggest that a large spacer between the initiator core and the initiation site is not necessary, despite concerns over steric hindrance

Table 1. Variety of initiators used in the polymerization processes and different DPs obtained for St-PBLGs, demonstrating the versatility of the technique.

Star	Initiator	DP_{theo}	Mn^a (kDa)	Mn^b (kDa)	DP^a	DP^b	Đ
SE1	Ethyl based	100	21.3	21.0	97	96	1.26
SE2		150	24.0	27.6	110	126	1.22
SE3		250	50.3	51.5	229	235	1.09
SH1	Hexyl based	75	16.4	-	75	-	1.25
SH2		150	23.9	23.6	109	108	1.23
SH3		250	51.5	52.7	235	240	1.17
SD1	DOOA based	75	15.7	16.9	72	77	1.13
SD2		100	22.2	24.1	101	110	1.23
SD3		150	33.2	31.1	152	142	1.10
SD4		200	40.4	41.6	185	190	1.12
SS1	Cyst based	200	43.1	-	196	-	1.22

[a)] Data obtained by SEC in DMF/LiBr (1 %) at 8 mg/mL. [b)] Data obtained by ^{1}H-NMR from the deprotected polymers by integrating the aromatic signal of the initiator. DP=degree of polymerization, Đ =polydispersity

a)

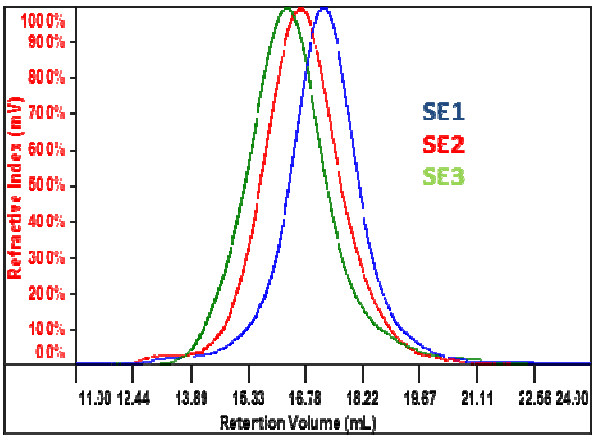

b)

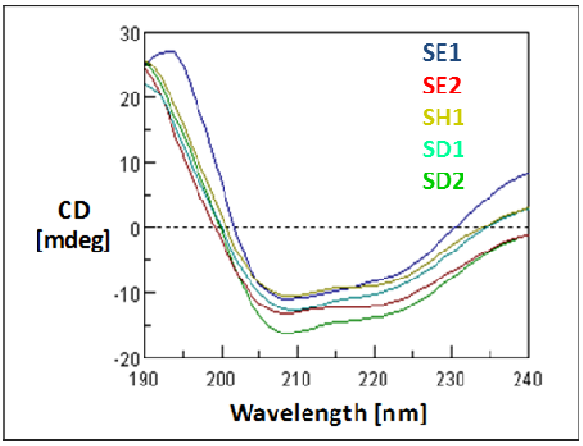

Figure 1. a) Selected GPCs from star-shaped polyglutamates (St-PBLG) in DMF (1 % LiBr) at 8 mg/mL. b) Circular Dichroism (CD) of benzyl protected star-shaped polyglutamates at 20 ºC in 1,1,1,3,3,3-hexafluoroisopropanol (HFIP) at 0.1 mg/mL.

The polymers were characterized using a number of physico-chemical analytical techniques, always yielding the desired molecular weight by Gel Permeation Chromatography (GPC) and proton Nuclear Magnetic Resonance ^{1}H-NMR. The data obtained from GPC and ^{1}H-NMR regarding DP was always consistent. Well-defined polymers were obtained even up to 50 kDa (Table 1). This is a highly significant fact and a major benefit offered by the technology we

are describing herein, since most star polypeptides described in the literature have not achieved high MW with narrow polydispersities.[25-34] CD spectra from the benzyl protected samples in HFIP showed the typical alpha helix conformation from PBLGs (Figure 1b).

All data obtained so far indicates an excellent control over the polymerization using these initiators, however, to fully demonstrate this fact, we endeavored to prove that the arms on the stars were of equal molecular weight and therefore with a low polydispersity.

To do this we employed the above-mentioned initiator bearing disulfide bonds on the arms that was very efficiently reduced by using DTT, thus releasing the individual arms allowing their monitoring by SEC. Remarkably, we were able to almost perfectly disassemble the star polymers to yield linear chains of 1/3 MW of the original star and with low polydispersities (<1.25) (Figure S1). This evidence, in addition to the expected MW of the stars from GPC and ^{1}H-NMR fully demonstrate that the star polymers synthesized have very similar length arms resulting from fast and efficient initiation and controlled propagation. Knowing that this synthesis of polyglutamate-based stars leads to homogenous material makes them much more favorable candidates to be used as drug delivery carriers or imaging probes.

In order to have a full understanding on the quality of the star polymers synthesized, the analysis of the deprotected polymers needed to be also performed. The benzyl protecting groups were removed using conventional methods already reported for linear polymers.[16-17] However, it was important to choose the correct deprotection approach depending on the initiator used. For example, to maintain the integrity of the DOOA core, a procedure using sodium hydroxide with previously optimized conditions capable of preserving the polyglutamate stereochemistry whilst at the same time completely removing the benzyl protecting groups was used. [16-17] Standard HBr/TFA acidic conditions were used in all other cases. The complete removal of the benzyl

protecting groups was certified by ^{1}H-NMR (7.4 ppm and 5.3 ppm) and the remaining aromatic signal observed, therefore, were assigned to the benzylic core of the star at 8.2 ppm (3 protons). Integration of this signal against those of glutamic acid provided the average number of units per chain and consequently the MW. In all cases, the MW obtained by ^{1}H-NMR was in agreement with that predicted by GPC for the benzyl protected precursor.

After deprotection, the expected random coil conformation of the PGA chains was observed in all samples when analyzed using Circular Dichroism (CD) (Figure 2). Finally, DLS (Dynamic Light Scattering) at 0.2 mg/mL showed particle sizes between 4-6 nm in hydrodynamic radius for all deprotected St-PGA, comparable to those obtained for their linear counterparts of similar MW (also in the range of 4-6 nm radius) (Figure 2).

To be sure that the enzyme-dependent biodegradability of the polyglutamate-based stars had not been compromised by the architecture, all polymers were incubated in presence of the lysosomal enzyme cathepsin B. The degradation rate or MW loss at different time points was monitored by GPC as described in the Experimental Section. As expected, the star polymers were found to be degraded by the lysosomal enzyme with similar kinetics independently of the MW and initiator used for the polymerization (Figure 3).

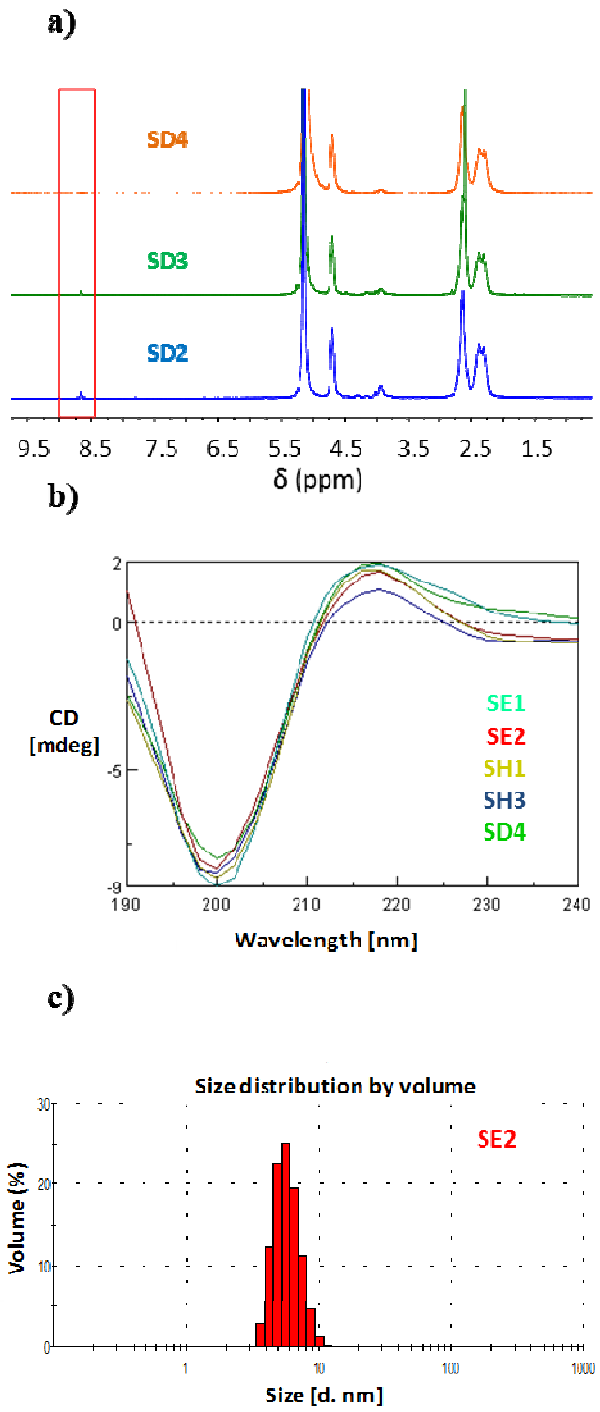

Figure 2. a) ^{1}H-NMR of St-PGAs of different molecular weights in D_2O. The red square is surrounding the benzyl core signals. b) CD of St-PGAs in PBS at 37 ºC at 1 mg/mL showing typical random coil conformation of PGA chains. c) Example of particle size obtained by DLS from St-PGAs at 0.2 mg/mL in PBS 7.4 at 25 ºC.

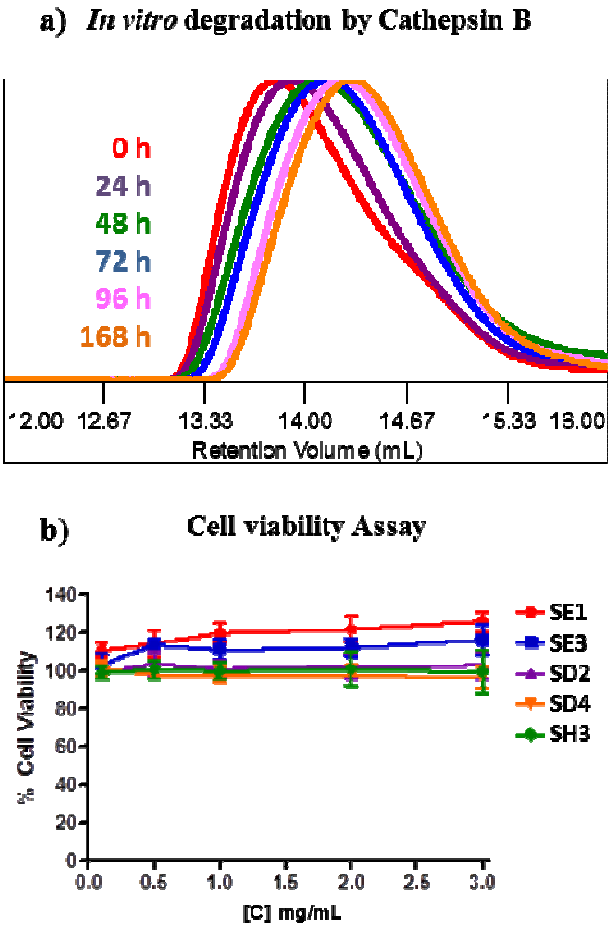

Figure 3. *In vitro* evaluation of the newly synthesized St-PGA (benzyl deprotected) carriers. a) Example of degradation profile by cathepsin B of SE3 polymer monitored by GPC in PBS at 3 mg/mL and at different time points. b) Toxicity assay against SHSY5Y cell line of different St-PGAs measure by MTS assay at 72 hours post-treatments.

Another key feature for the validation of the newly synthesized 3-arm star shaped polymers as potential drug delivery carriers or imaging probes is their toxicity in cell cultures. To this respect, 72 hours MTS assays were performed against SHSY5Y human derived neuroblastoma cell line as well as in HUVEC human umbilical vein endothelial cells. Polymers were found to be non-toxic up to 3 mg/mL (Figure 3, and Figure S2).

For macromolecular therapeutics and nano-sized drug delivery systems, fluorescent labeling is commonly applied to allow intracellular trafficking studies, conjugate cell-specific localization and/or *in vivo* fate and PK. Probes such as the fluorophore Oregon Green (OG) have been extensively reviewed for cellular studies to determine cell uptake and binding.[32-34] To this aim, the conjugated probe must fulfill some requirements such as high stability of the probe itself as well as stability of the linkage point to ensure adequate carrier monitoring. On the other hand, the minimal probe loading is desirable in order to avoid data misinterpretation due to changes in the polymer conformation resulting from changes in charge and solubility. Thus, a minimal amount of OG (0.8 % mol) was successfully conjugated to the star-shaped polyglutamates using diisopropylcarbodimide (DIC) / Hydroxybenzotriazole (HOBt) as carboxylic acid activators (Scheme S1).

Flow cytometry (cell uptake and binding) together with live-cell confocal microscopy analysis (subcellular fate and pathway) in SHSY5Y human derived neuroblastoma cell line, were used to study cellular trafficking of the OG-labeled star-shaped polymers (Figure 4). Flow cytometry experiments were carried out at different temperatures, 37 °C (to measure the total uptake) and 4 °C (to measure cell binding) in order to determine the presence of energy dependent or non-dependent internalization mechanisms, such as endocytosis or diffusion, respectively. It is worth mentioning that all experiments were done in presence of the cathepsin B inhibitor CA-047 in order to avoid the degradation of the polyglutamic acid chains along the incubation periods.

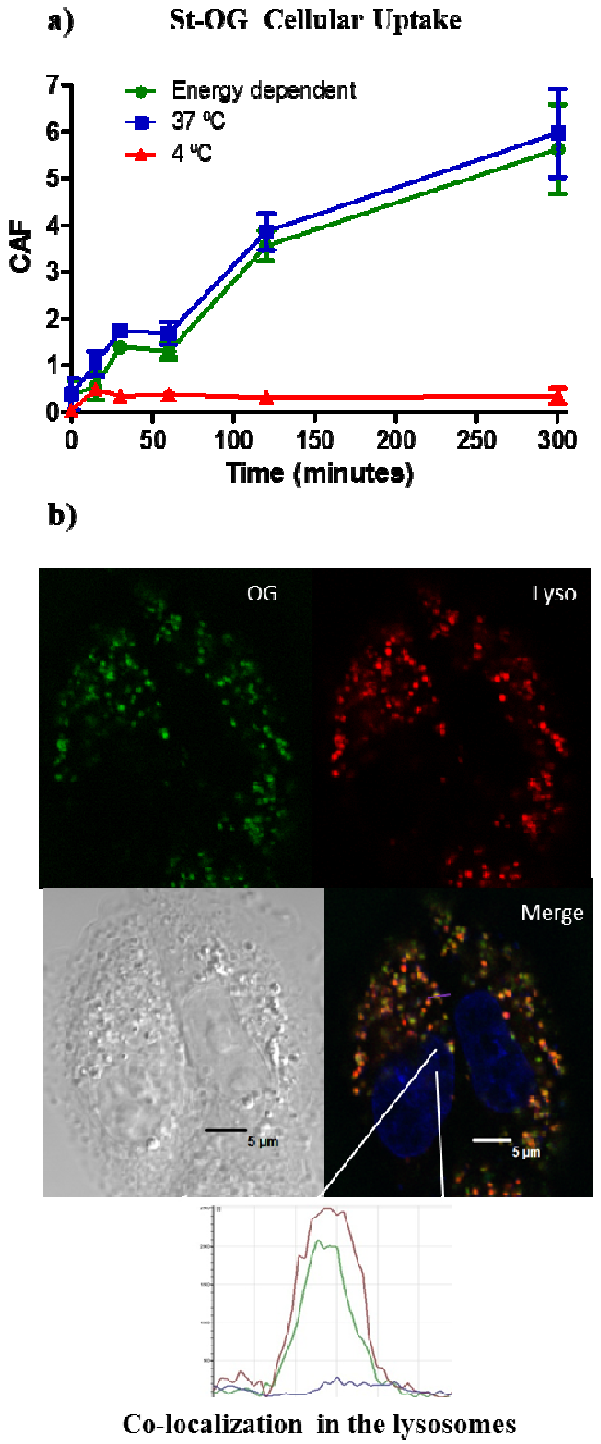

Figure 4. *In vitro* evaluation of the newly synthesized carriers. a) Uptake study by flow cytometry of a star-shaped fluorescently labeled PGA (SE3 deprotected) in SHSY5Y cell line. Experiment at 4 ºC excludes the energy dependent mechanisms. The different among the uptake

profile at 4 and 37 degrees (so-called "Energy-dependent" uptake) is also represented. CAF: Cell associated fluorescence= % positive cells*mean fluorescence/100. The CAF represented corresponds to the difference between CAF obtained with treated cells and CAF from untreated control cells. b) Confocal image of the uptake at 2 hours post-treatment of a star-shaped PGA in SHSY5Y cell line following a pulse-chase experiment, with co-localization histogram. Co-localization with the lysosomal marker Lysotracker Red was observed.

Live-cell confocal imaging allows visualizing trafficking between multiple compartments within individual living cells over time, avoiding any possible artifacts derived from fixation protocols.[34] Results from both techniques clearly showed an energy-dependent mechanism of internalization due to the absence of uptake at 4 ºC as observed by flow cytometry. This was further confirmed with the confocal microscopy studies at 2 hours post-treatment with an OG labeled polymer in SHSY5Y cells following a pulse-chase experiment, where co-localization in the lysosomes was observed upon the use of lysosomal marker Lysotracker Red (Figure 4b).

Interestingly, the St-PGA-OG showed a significant increase in cell uptake at 5 hours when compared with linear-PGA-OG conjugate of similar MW (Figure 5). This might be attributed to the inherent properties assigned to the star-shaped polymers. As general basis, star polymers have a more compact structure, presumably with globular shape, and have large surface areas, increased concentrations of functional end groups for polymers with equal molecular weight, and unique rheological properties which make them optimal platforms for drug delivery and imaging among other biological applications.[35-36]

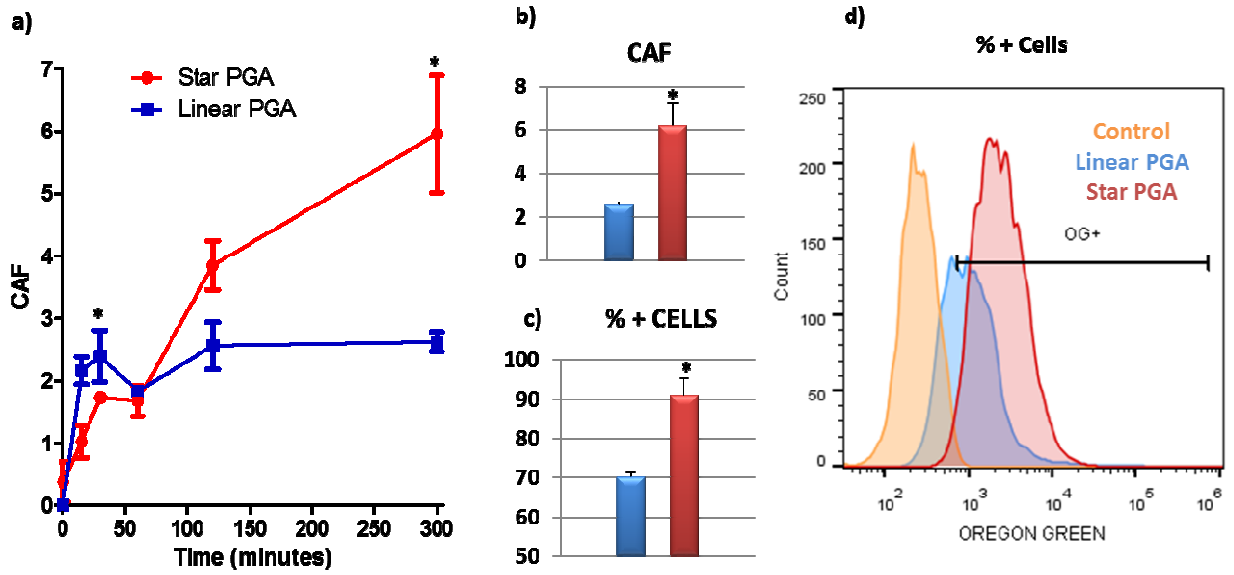

Figure 5. Uptake study of St-PGA (SE3, deprotected) in comparison with linear PGA of similar MW (around 250 GAU). a) CAF of both polymers over time. b) CAF of both polymers at 5 hour time point showing significant differences when statistics was performed using one-way ANOVA. p*< 0.05. c) % of positive (+) cells to Oregon Green (OG) fluorescence, comparison of both polymers at 5 hour time point showing as expected statistical differences. p*< 0.05. d) % of positive cells representation comparing both polymers together with the control used (cell autofluorescence).

To further validate the synthesized nanocarriers, *in vivo* biodistribution as well as pharmacokinetic profiles (PK) were obtained by radioactivity measurements. For that purpose, a gamma emitting radionuclides ^{111}In was introduced into the star-shaped PGAs through complexation chemistry. In order to accomplish a stable complexation of the metal radioisotope, the incorporation of bifunctional chelating agents into the polymer backbone is required. The most commonly used chelating agents for ^{111}In are based on polyamine carboxylic acids such as diethylene triamine pentaacetic acid (DTPA), 1,4,7,10-tetraazacyclododecane-1,4,7,10-

tetraacetic acid (DOTA), or 1,4,7-triazacyclododecane-1,4,7-tetraacetic acid (NOTA). For the biodistribution of radiolabeled PGA based architectures, DOTA derivative chelating agent with a free amine group suitable for conjugation (DO_3A-NH_2) was selected. It is well-known that, DO_3A-NH_2 forms stable complexes with several M^{2+} and M^{3+} ions such as ^{68}Ga or ^{111}In. Therefore, 20 % mol GAU of DO_3A-tBu-NH_2 was effectively conjugated via amide bond to a St-PGA_{110} (Đ 1.23) following the strategy depicted in the Scheme S2.

Conjugation efficiency was almost quantitative (since 10 % mol GAU was pursued) with a reasonable mass yield of 75 %. The percentage of modification was calculated according to ^{1}H-NMR analysis by comparing the corresponding integral of the CH alpha of PGA (4.24 ppm) with the 27 protons of the tBu groups at 1.40 ppm. The tBu groups were then easily deprotected using the mixture CH_2Cl_2/TFA (3/2, v/v). Finally, the St-PGA-DO_3A polymer was labelled with ^{111}In as described previously. Radiochemical yields were ≥ 85 % for St-PGA-DO_3A-^{111}In in all synthesis. In the exclusion molecular purification step (Figure 3S), the first 5 fractions were discarded and the next 3 fractions, containing the maximum specific activity of St-PGA-DO_3A-^{111}In, were collected and used for further experiments.

Animal experiments to test the biodistribution and PK profile were then carried out with i.v. injected doses between 37 KBq and 2.5 MBq of ^{111}In-labelled polymers (1-20 µg/g body weight) and monitored up to 24 hours (4-5 mice were sacrificed per time point 0.5, 1, 2, 4, 8 and 24 hours). Blood and organs were extracted and radioactivity was measured ex vivo in the gamma counter.

According to the results obtained from the biodistribution, where the higher percentage of injected dose (ID) corresponded to the kidneys, it can be concluded that these new polypeptide

architectures follow renal excretion profiles with no specific accumulation in any organ (Figure 6).

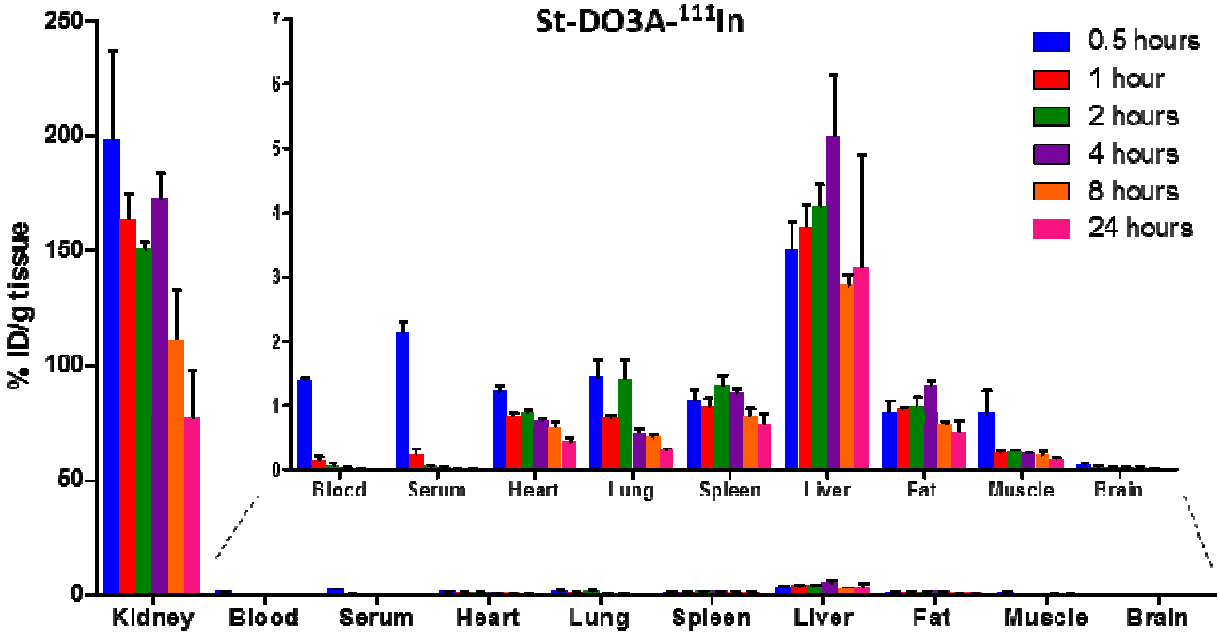

Figure 6.1 St-DO_3A-^{111}In biodistribution. Data expressed as normalized % ID per gram of tissue at different time points.

The biodistribution profile obtained for St-PGA was then compared with the one obtained for its linear counterpart of similar MW (100 GAU, Đ: 1.20).[37] The biodistribution of linear PGA was previously performed using ^{68}Ga radioisotope, therefore, only short times (up to 3 hours) could be recorded due to radionuclide decay (about 68 min for ^{68}Ga). If short time points (0.5 h, 1 h and 2 h) of the % ID/g tissue of PGA-DO_3A-^{68}Ga and St-DO_3A-^{111}In are compared, a general greater accumulation in all the organs of star shaped polymer is observed, in comparison with the one found in the linear PGA construct as shown in Figure 7.

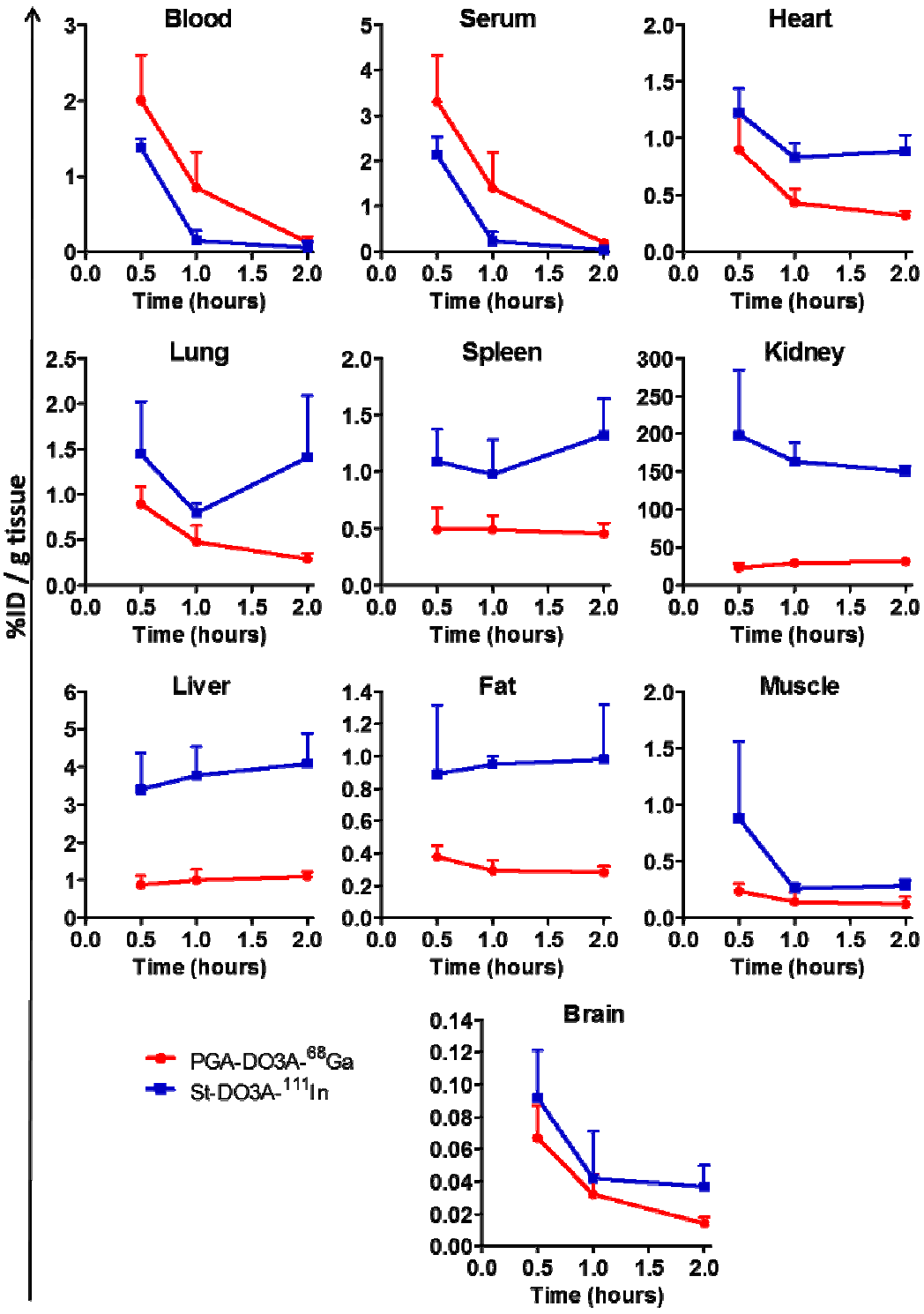

Figure 7.2 Normalized data of radioactivity signal of each organ respect the injected dose (ID) per gram of tissue, of St-PGA compared with it linear counterpart of similar MW. Time course experiment.

Although the plasmatic profiles are similar for both compounds, differences can be drawn when we compared the PK parameters obtained for PGA-DO_3A-^{68}Ga with St-PGA-DO_3A-^{111}In. The linear polymer was not detected after 4 hours post administration. Their biological or terminal half-life estimated resulted to be 13 times higher for the star polymer, this fact could be in part attributed to the use of different radionuclides for the study. The use of ^{111}In allowed to study and estimate the PK parameters of the stars providing results more reliable due to the higher semidesintegration period for ^{111}In (2.1 days) compared to ^{68}Ga (68 min).

In the case of the two compartment model a number of volume terms can be defined. V_{ss} is the appropriate volume of distribution (Vd) when plasma concentrations are measured in steady state conditions. This V_{ss} value is about 9 times higher for the star polymer compared to the linear one, meaning a greater distribution of the carrier. The Clearance value (Cl) from the central compartment is slightly higher also in the star-shaped polymer (18.35 vs 11.77 mL/h for linear PGA). The renal clearance value of inulin (a model compound that is excreted only by glomerular filtration and is not subject to tubular secretion or re-absorption) has being established to be around 20 mL/h by in FVB mice.[38] This value is really close to the value obtained for the star polymer. Thus it could be claimed that the polymer is cleared out only by glomerular filtration. In the case of linear PGA, the value is slightly smaller. This could be explained by the binding of the compound to plasmatic proteins, reducing the glomerular filtration, or if the linear polymer could be reabsorbed in the tubules.

4. Conclusions

As addressed in the introduction, there is a current need and an increasing tendency in the polymer field for the construction of novel and versatile architectures of non-toxic and biodegradable polymers that can meet with FDA approval criteria. These polymers require

properties such as high molecular weights (to take advantage of the EPR effect and prevent rapid renal clearance), have predictable structure and conformation in solution and have high drug loading capacity whilst maintaining good aqueous solubility. We have reported here a controlled living polymerization approach to obtain polyglutamate-based star shaped polymers based on our recently described ROP of NCAs with novel non-nucleophilic initiators, a sign of its versatility.[16-17] Not only this, but the stars had well-defined structures with adjustable MWs and low dispersities (Đ<1.3).

Herein, we have also described a method that gives very convincing evidence that the arms on the stars were of equal MW by using reducible initiators containing disulfide bonds. We have highlighted this as a highly significant result when considering new polymer carriers as drug delivery systems or imaging probes due to the need for homogeneity in these materials. Our results also show that these St-PGAs are biodegradable in presence of lysosomal enzymes, non-toxic against model cell lines up to 3 mg/mL concentration and follow energy-dependent cell internalization mechanisms as demonstrated by flow cytometry and live-cell confocal imaging experiments. Importantly, with a 3-fold cell uptake for St-PGA when compared to linear PGA. Biodistribution and pharmacokinetic data suggest renal excretion profiles with no specific accumulations in any organs. Moreover, when compared with linear PGA of similar MW, the star-shaped polymer shows longer retention times, and greater distribution. All this data validates them as potential drug delivery carriers or imaging probes amongst other applications.[35-36]

ASSOCIATED CONTENT

Supporting Information. Additional protocols and characterization data of the different 3-arm star initiators can be found in the Supporting Information. This material is available free of charge via the Internet at http://pubs.acs.org.

AUTHOR INFORMATION

Corresponding Author

* Dr. María J. Vicent

Centro de Investigación Príncipe Felipe, Polymer Therapeutics Lab.,

Av. Eduardo Primo Yúfera 3, E-46012 Valencia (Spain)

Tel.: +34 963289680; Fax: +34 963289701

E-mail: mjvicent@cipf.es

Author Contributions

The manuscript was written through contributions of all authors. All authors have given approval to the final version of the manuscript

ACKNOWLEDGMENT

This work was supported by grants from the Spanish Ministry (MICINN-MINECO) (CTQ2010-18195/BQU, SAF2013-44848-R, FPU grant AP2010-4592 and ERA-Chemistry EUI2008-3904). The authors would like to thank the technician Maria Helena Ferrandis and Dr Ana Armiñan for helpful discussions on the biological experiments.

REFERENCES

1. Duro-Castano, A.; Conejos-Sánchez I.; Vicent, M. J. *Polymers* **2014,** 6, (2), 515-551.
2. Seymour, L. W.; Miyamoto, Y.; Maeda, H.; Brereton, M.; Strohalm, J.; Ulbrich, K.; Duncan, R. *Eur J Cancer* **1995,** 31A, (5), 766-70.
3. Matsumura, Y.; Maeda H. *Cancer Res* **1986,** 46, (12 Pt 1), 6387-92.
4. Maeda, H.; Fang, J.; Inutsuka, T.; Kitamoto, Y. *Int Immunopharmacol* **2003,** 3, (3), 319-28.
5. Deming, T. J. *Journal of Polymer Science Part A: Polymer Chemistry* **2000,** 38, (17), 3011-3018.
6. Kricheldorf, H. *Angew Chem Int Ed* **2006,** 45, (35), 5752-84.

7. Hadjichristidis, N.; Iatrou, H.; Pitsikalis, M.; Sakellariou, G. *Chem Rev* **2009,** 109, (11), 5528-78.
8. Leuchs, H.; Geiger, W. *Dtsch Chem Ges* **1908,** 41, 1721.
9. Leuchs, H.; Manasse, W. *Dtsch Chem Ges* **1907,** 40, 3235.
10. Leuchs, H. *Dtsch Chem Ges* **1906,** 39, 857.
11. Aliferis, T.; Iatrou, H.; Hadjichristidis, N.. *J. Polym Sci Part A: Polym Chem* **2005,** 43, 4670-4673.
12. Dimitrov, I.; Schlaad, H. *Chem Commun (Camb)* **2003**, (23), 2944-2945.
13. Deming, T. J. *Nature* **1997,** 390, (6658), 386-9.
14. Lu, H.; Cheng, J. *J Am Chem Soc* **2007,** 129, (46), 14114-14115.
15. Vayaboury, W.; Giani, O.; Cottet, H.; Deratani, A.; Schué, F. *Macromolecular Rapid Communications* **2004,** 25, (13), 1221-1224.
16. Conejos-Sanchez, I.; Duro-Castano, A.; Birke, A.; Barz, M.; Vicent, M.J. *Polymer Chemistry* **2013,** 4, (11), 3182-3186.
17. Vicent, M.J.; Barz, M.; Canal, F.; Conejos-Sánchez, I.; Castaño, Duro-Castano, A.. *P201131713* **2012**.
18. Klok, H.; Hernández, J. R.; Becker, S.; Müllen K. *Journal of Polymer Science Part A: Polymer Chemistry* **2001,** 39, (10), 1572-1583.
19. Inoue K.; Horibe S.; Fukae, M.; Muraki, T.; Ihara E.; Kayama H. *Macromolecular Bioscience* **2003,** 3, (1), 26-33.
20. Inoue, K.; Sakai, H.; Ochi, S.; Itaya, T.; Tanigaki, T. *Journal of the American Chemical Society* **1994,** 116, (23), 10783-10784.
21. Aliferis T.; Iatrou, H.; Hadjichristidis N.; Messman J.; Mays J. *Macromolecular Symposia* **2006,** 240, (1), 12-17.
22. Karatzas, A.; Bilalis, P.; Iatrou, H.; Pitsikalis, M.; Hadjichristidis, N. *Reactive and Functional Polymers* **2009,** 69, (7), 435-440.
23. Huang, H.; Li, J.; Liao, L.; Li, J.; Wu, L.; Dong, C.; Lai, P.; Liu, D. *European Polymer Journal* **2012,** *48* (4), 696-704.
24. Byrne, M.; Victory, D.; Hibbitts, A.; Lanigan, M.; Heise, A.; Cryan, S.-A. *Biomaterials Science* **2013,** *1* (12), 1223-1234.
25. Byrne, M.; Thornton, P. D.; Cryan, S. A.; Heise, A. *Polymer Chemistry* **2012,** *3* (10), 2825-2831.
26. Higashi, N.; Uchino, A.; Mizuguchi, Y.; Niwa, M.. *Int J Biol Macromol* **2006,** *38* (2), 120-5.
27. Hua, C.; Dong, C. M.; Wei, Y. *Biomacromolecules* **2009,** *10* (5), 1140-8.
28. Sulistio, A.; Lowenthal, J.; Blencowe, A.; Bongiovanni, M. N.; Ong, L.; Gras, L.; Zhang, X.; Qiao, G. G.,. *Biomacromolecules* **2011,** 12, (10), 3469-3477.
29. Sulistio, A.; Blencowe, A.; Widjaya, A.; Zhang X. ; Qiao, G. G. *Polymer Chemistry* **2012,** 3, (1), 224-234.
30. Sulistio, A.; Gurr, P. A.; Blencowe, A. ; Qiao, G.G. *Australian Journal of Chemistry* **2012,** 65, (8), 978-984.
31. Xing, T.; Lai, B.; Ye, X.; Yan, L. *Macromolecular Bioscience* **2011,** 11, (7), 962-969.
32. Richardson, S. C.; Pattrick, N. G.; Lavignac, N.; Ferruti, P.; Duncan, R. *J Control Release* **2010,** 142, (1), 78-88.
33. Richardson, S. C.; Wallom, K. L.; Ferguson, E. L.; Deacon, S. P.; Davies, M. W.; Powell, A. J.; Piper, R. C.; Duncan R.. *J Control Release* **2008,** 127, (1), 1-11.

34. Seib, F. P.; Jones, A. T. ; Duncan, R. *Journal of Controlled Release* **2007,** 117, (3), 291-300.
35. Hadjichristidis, N.; Pitsikalis, M.; Iatrou, H.; Driva, P.; Sakellariou, G.; Chatzichristidi, M., 6.03 - Polymers with Star-Related Structures: Synthesis, Properties, and Applications. In *Polymer Science: A Comprehensive Reference*, Möller, K. M., Ed. Elsevier: Amsterdam, 2012; pp 29-111.
36. Hadjichristidis, N.; Pitsikalis, M.; Iatrou, H., Polymers with Star-Related Structures. In *Macromolecular Engineering*, Wiley-VCH Verlag GmbH & Co. KGaA: 2007; pp 909-972.
37 Conejos-Sánchez, I.; Cardoso, I.; Oteo-Vives, M.; Romero-Sanz, E.; Paul, A.; Sauri, A. R.; Morcillo, M. A.; Saraiva, M. J.; Vicent, M. J. *Journal of Controlled Release* **2015,** 198, (0), 80-90.
38 Eisner, C.; Faulhaber-Walter, R.; Wang, Y.; Leelahavanichkul, A.; Yuen, P. S. T.; Mizel, D.; Star, R. A.; Briggs, J. P.; Levine, M.; Schnermann, J. *Kidney Int* **2010,** 77, (6), 519-526.

Table of contents

Amino acid building blocks and polypeptide structural characteristics represent a good opportunity to overcome some of the well-known limitations of the current drug delivery carriers such as their biodegradability, biocompatibility and multifunctionality, making them good candidates for different applications in relevant areas such as biomedicine and biotechnology. The present article reports on the development of synthetic pathways to a plethora of functional 3-arm star-shaped polyglutamates with well-defined structures, adjustable molecular weights and low dispersity (Đ= <1.3) by applying the ring opening polymerization (ROP) of N-carboxyanhydrides (NCA). Preliminary *in vitro* and *in vivo* evaluation showed advantages over their linear counterparts regarding cell uptake and PK *in vivo*, confirming their potential use as carriers in nanomedicine applications.